

Electron Spin Resonance Study of Heterocycles.

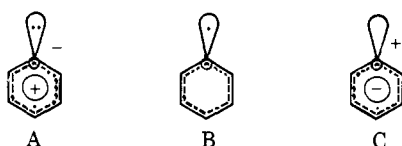
I. Pyridyl Radicals

Paul H. Kasai* and D. McLeod, Jr.

Contribution from the Union Carbide Corporation, Tarrytown Technical Center, Tarrytown, New York 10591. Received May 27, 1971

Abstract: Electron spin resonance (esr) spectra of 2-, 3-, and 4-pyridyl radicals generated within argon matrices by a photoelectron transfer process are presented and discussed. The radicals are all found to be σ radicals, and the observed coupling constants are in good agreement with those predicted by a self-consistent field molecular orbital calculation. The radicals are also found to decompose when irradiated with uv light, resulting in a rupture of the aromatic ring. The esr spectra showing these photolysis sequences are also presented and discussed.

When a peripheral σ bond is cleaved homolytically from an aromatic system such as benzene or pyridine, the resulting aryl radical is expected to possess one of the three electronic states A-C. The phenyl



radical has been shown to be a σ radical (case B) by Porter and Ward¹ who investigated its electronic spectrum using a flash photolysis technique, by Bennett, Mile, and Thomas² who studied the esr spectra of the radicals trapped in various matrices at 77°K, and more recently by Kasai, Hedaya, and Whipple³ who made a more detailed analysis of the esr spectrum of the radicals generated in an argon matrix at ~4°K.

An obvious but extremely interesting extension of such study would be to examine the electronic ground states of various pyridyl radicals. 2-Pyridyl radical has been identified in γ -irradiated pyridine and shown to be a σ radical by Bower, McRae, and Symons.⁴ We began our study with attempts to generate 2-, 3-, and 4-pyridyl radicals by photolysis of the corresponding iodides in argon matrices. The esr spectra obtained, however, were mostly due to radicals which could result only from a process involving a rupture of the aromatic ring. Subsequently we have succeeded in generating and obtaining the esr spectra of all three pyridyl radicals by the method of dissociative electron capture within an argon matrix at ~4°K.⁵ 2-, 3-, and 4-pyridyl radicals so generated are all found to be σ radicals and all are found to undergo photolysis when exposed to uv light, resulting in a disappearance of the original spectra and an appearance of the spectra identical with those obtained by direct photolysis of the iodides. If pyridyl radicals are indeed σ radicals, another interesting aspect is the extent of the interaction between the semi-filled orbital of the broken bond and the lone-pair orbital of the nitrogen. Interaction between two "local-

ized" orbitals through space or bonds within a molecule has been the subject of many theoretical studies.⁶

Presented in this report are the detailed analyses of the esr spectra of pyridyl radicals generated by dissociative electron capture and the description of their photolysis sequences. Results of the molecular orbital calculations, the extended Hückel theory (EHT), and a self-consistent field method (INDO), performed in order to substantiate the spectroscopic assignments and to elucidate the photolysis sequences, are also presented and discussed.

Experimental Section

The details of the liquid helium dewar and an X-band esr spectrometer system which allows the trapping of reactive species and measurement of their esr spectra at ~4°K have been previously described.⁷ The argon matrix is formed on a flat spatula shaped sapphire rod which can be rotated about its long axis and moved vertically in and out of the esr cavity (Figure 1). Pyridyl halides were introduced through the vapor sample inlet, and Na atoms, when required, were vaporized from a resistively heated stainless-steel cell. Irradiation of the matrix was done through the side quartz window, and a high-pressure mercury lamp (GE AH-6) combined with an appropriate filter was the light source. In the following text "uv irradiation" refers to the usage of a uv filter (Corning 7-54) and "irradiation with yellow light" refers to the usage of a sharp cutoff filter (Corning 3-70) which cuts off all the light below 5000 Å. The direct photolysis by uv was possible only with pyridyl iodides. We shall first discuss the spectra of pyridyl radicals generated by the process of dissociative electron capture and then present and analyze the spectra obtained when the pyridyl radicals are photolyzed further or when the iodides are photolyzed directly. In every case the spectrometer frequency locked to the loaded sample cavity was 9.430 ± 0.001 GHz.

During the course of studying 3-pyridyl radicals, the synthesis of 4-deuterio-3-iodopyridine became desirable. 4-Deuteriopyridine was, therefore, prepared from 4-bromopyridine by the method of Bak, *et al.*⁸ The monodeuterated pyridine was then converted to 3-iodopyridine by refluxing it with iodine in fuming, nondeuterated sulfuric acid at 300-320° (!), a method reported by Rodewald and Plazek.⁹ The nmr analysis showed that the product purified by distillation was all 4-deuterio-3-iodopyridine. Apparently no deuterium-hydrogen exchange occurs at the 4 position during the iodination.

Esr Spectra of Pyridyl Radicals

It has been demonstrated that charged species can be generated and trapped within a rare-gas matrix by trapping both electron-donating species and accepting

(1) G. Porter and B. Ward, *Proc. Roy. Soc., Ser. A*, **287**, 457 (1965).
 (2) J. E. Bennett, B. Mile, and A. Thomas, *ibid.*, **293**, 246 (1966).
 (3) P. H. Kasai, E. Hedaya, and E. B. Whipple, *J. Amer. Chem. Soc.*, **91**, 4364 (1969).
 (4) H. J. Bower, J. A. McRae, and M. C. R. Symons, *J. Chem. Soc. A*, 2696 (1968).
 (5) P. H. Kasai and D. McLeod, Jr., *J. Amer. Chem. Soc.*, **92**, 6085 (1970).

(6) See, for example, R. Hoffmann, *Accounts Chem. Res.*, **4**, 1 (1971).
 (7) P. H. Kasai, E. B. Whipple, and W. Weltner, Jr., *J. Chem. Phys.*, **44**, 2581 (1966).
 (8) B. Bak, L. Hansen, and J. Rastrup-Andersen, *ibid.*, **22**, 2013 (1954).
 (9) Z. Rodewald and E. Plazek, *Ber. Deut. Chem. Ges.*, **70**, 1159 (1937).

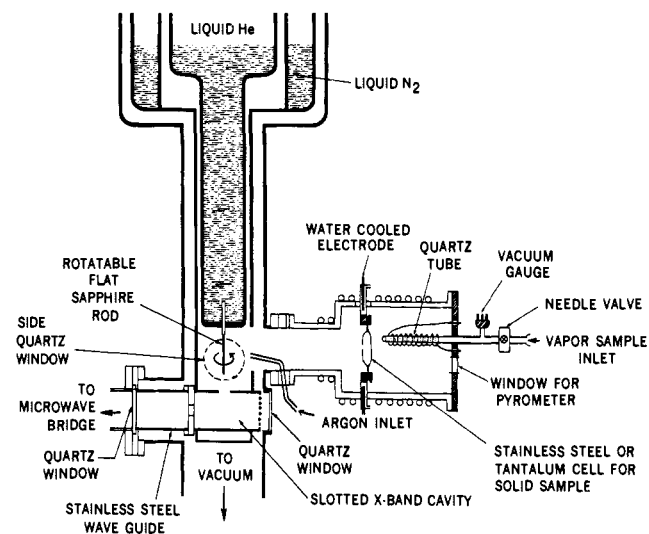


Figure 1. Cross section of the matrix isolation cryostat used. Pyridyl halides were introduced through the vapor sample inlet, while Na was vaporized from the resistively heated stainless steel cell.

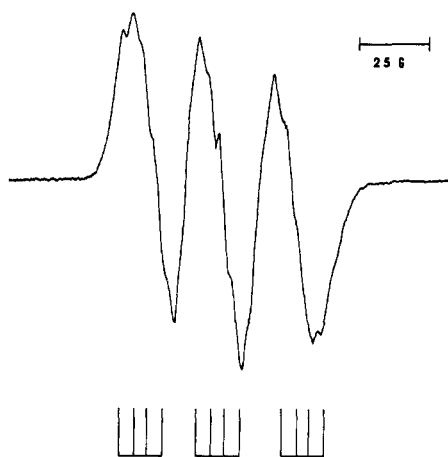
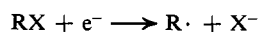


Figure 2. ESR spectrum of an argon matrix containing 2-chloropyridine and Na atoms obtained after irradiation with yellow light and the splitting pattern based upon the assessed isotropic coupling constants.

species of suitable choice within a same matrix and then promoting an electron transfer between them by photoexcitation.¹⁰ It is also known that dissociative electron capture is a particularly prevailing process in radiation chemistry of organic halides.



We, therefore, prepared argon matrices containing Na atoms (electron donors) and pyridyl halides (electron acceptors). The mole ratio of Na:pyridyl halide:argon was roughly 1:10:1000. Prior to photoexcitation every matrix appeared deep purple owing to the sodium "D line" resonance transitions and showed an esr spectrum consisting of a sharp quartet due to Na atoms ($I = 3/2$, $A \cong 330$ G) and a weak broad signal centered about the position corresponding to $g = 2.00$. Irradiation of these matrices with yellow light for 10 min resulted in complete bleaching of the purple color, disappearance of the Na quartet signal, and a several-fold increase of the signal at $g = 2.00$. It should be

(10) P. H. Kasai, *Phys. Rev. Lett.*, **21**, 67 (1968); *Accounts Chem. Res.*, **4**, 329 (1971).

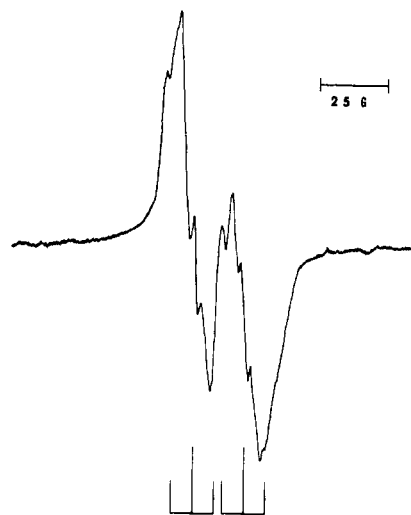


Figure 3. ESR spectrum of an argon matrix containing 3-chloropyridine and Na atoms obtained after irradiation with yellow light and the splitting pattern based upon the assessed isotropic coupling constants.

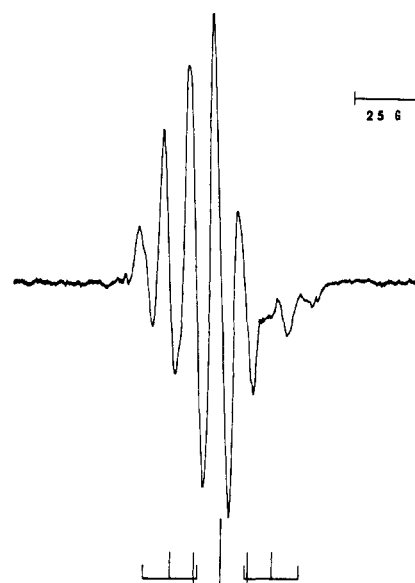
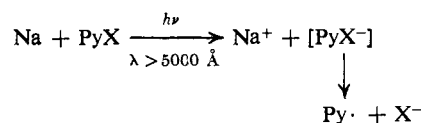


Figure 4. ESR spectrum of an argon matrix containing 4-iodopyridine and Na atoms obtained after irradiation with yellow light and the splitting pattern based upon the assessed isotropic coupling constants.

emphasized that no change occurs when a matrix containing Na atoms or pyridyl halide alone is irradiated with the yellow light. Figures 2-4 show the spectra obtained after the photoexcitation when 2-chloropyridine, 3-chloropyridine, and 4-iodopyridine, respectively, were used as acceptors. The prominent structure resolved in these figures is much too large to be attributed to the hyperfine structures (hfs) expected for the π -type anion radicals of pyridyl halides. The spectra are, therefore, assigned to the σ -type 2-, 3-, and 4-pyridyl radicals, respectively, which had resulted from the dissociation of the anions.



Generally speaking the hyperfine structure of the esr

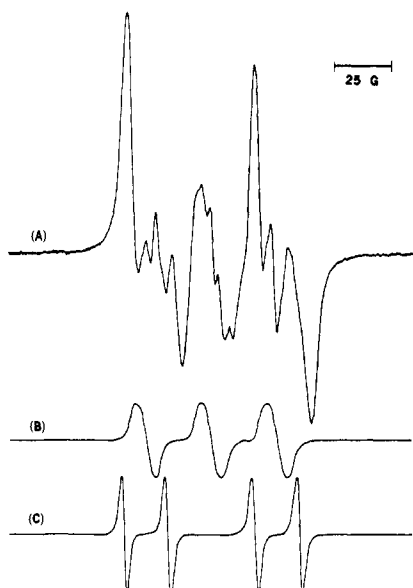


Figure 5. (A) ESR spectrum of an argon matrix containing 2-iodopyridine alone obtained after irradiation with uv. It consists of the triplet (B) due to 2-pyridyl radicals, and the doublet-of-doublet signal (C) as indicated.

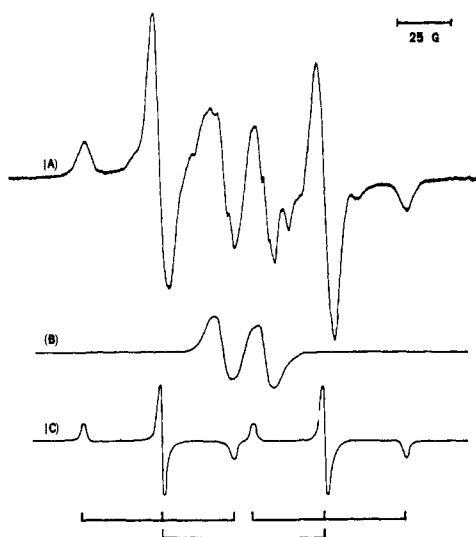


Figure 6. (A) ESR spectrum of an argon matrix containing 3-iodopyridine alone obtained after 10 min of uv irradiation. It consists of the doublet (B) due to 3-pyridyl radicals and the doublet-of-triplet spectrum (C) as indicated. The unique shape of the triplet pattern of C results from an axially symmetric but highly anisotropic coupling tensor ($A_{\parallel} \gg A_{\perp} \cong 0$) to the ^{14}N nucleus.

spectra of radicals immobilized within a polycrystalline matrix is broadened and complicated by the anisotropy of the hyperfine interaction. In the present situation an additional broadening is expected from the cleaved halide ion which possesses a nuclear magnetic moment and is surely expected to be within a range close enough to affect the esr signal. The spectra shown in Figures 2 and 3 are clearly better resolved than the spectra obtained from 2- and 3-iodopyridines and reported in our preliminary communication.⁵ The improved resolution obtained with chloropyridines is attributed to a smaller magnetic moment of chlorine nucleus (0.82 nuclear magneton) relative to that of iodine (2.79 nuclear magneton) and/or to a larger separation possible

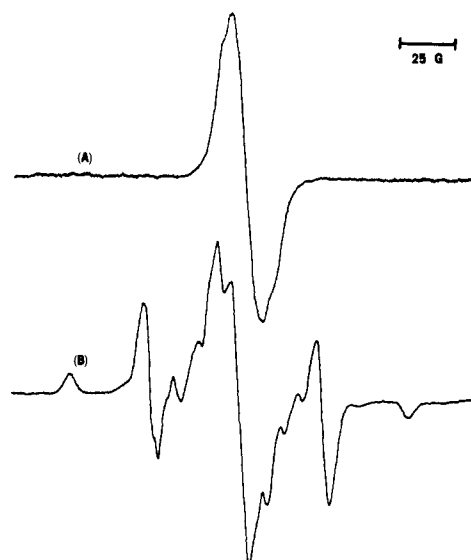


Figure 7. ESR spectrum of an argon matrix containing 4-deuterio-3-iodopyridine obtained (A) after 10-min irradiation with yellow light and (B) after 10-min irradiation with uv.

between the resulting pyridyl radical and halide ion owing to a smaller mass of chlorine atom.

Depicted below the observed spectra in Figures 2-4 are the patterns based upon the isotropic coupling constants assessed from these completely or partially resolved structures. The smaller coupling constants, the quartet structure of 2-pyridyl radicals, and the triplet structure of 3-pyridyl radicals were actually assessed from the spectra of partially photolyzed matrices which showed the signals of remaining pyridyl radicals with improved resolution (see the following section and Figures 5-7). The assignments of the coupling constants are tabulated in Table I and compared with those

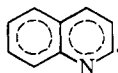
Table I. g Values (Observed) and Coupling Constants A (Observed and Calculated) of Pyridyl Radicals

Radical (g values)	Nucleus	A , G		
		Obsd	INDO	EHT
2-Pyridyl (2.002 ± 0.001)	N	29 ± 1	29.3	3.9
	$^{13}\text{C}(2)$	170^a	237	38.4
	H(3)		5.6	2.5
	H(4)	10 ± 1	8.6	4.6
	H(5)	6 ± 1	6.1	3.0
	H(6)		1.5	0.0
3-Pyridyl (2.002 ± 0.001)	N		1.1	0.0
	H(2)	8 ± 2	10.7	2.5
	H(4)	19 ± 1	18.8	7.1
	H(5)		3.6	2.5
	H(6)	8 ± 2	8.1	5.6
	4-Pyridyl (2.002 ± 0.001)	N		1.1
H(2), H(6)	10 ± 1	8.6	4.6	
	H(3), H(5)	19 ± 1	18.3	4.6

^a $^{13}\text{C}(2)$ coupling constant reported in ref 4 for 2-pyridyl radicals identified in γ -irradiated pyridine.

predicted by the INDO and EHT molecular orbital calculations. These calculations also showed that 2-, 3-, and 4-pyridyl radicals are all σ radicals. The excellent agreement obtained between the observed coupling constants and those calculated by a self-consistent field method (INDO) for each pyridyl radical is a strong substantiation of the mechanism and the assignment proposed.

Thus, the triplet pattern with a spacing of 29 G seen with the 2-pyridyl radical (Figure 2) is attributed to the hfs due to the ^{14}N nucleus. It indicates the existence of a "benzyne" type interaction between the broken nonbonding orbital and the lone-pair orbital of the nitrogen. The esr signal detected in γ -irradiated pyridine was originally assigned to pyridine cations¹¹ but was later reinterpreted by Bower, *et al.*,⁴ as arising from 2-pyridyl radicals. In a full support of the latter assignment, the spectrum of 2-pyridyl radicals obtained here is almost identical with that seen with γ -irradiated pyridine. The assignment of the coupling constants of 10 and 6 G to the protons 4 and 5, respectively, is based upon the following facts. (1) Bower, *et al.*,⁴ showed by deuterium substitution that the proton 4 in 2-pyridyl radical has the largest proton coupling. (2) The esr spectrum of 2-quinolyl radicals appears only as a triplet



of doublets, the spacings being 30 and 9 G, respectively.¹²

The large doublet pattern of 19-G separation observed with the 3-pyridyl radical (Figure 3) is assigned to the hfs due to the proton 4. This assignment is firmly confirmed by the spectrum of 4-deuterio-3-pyridyl radicals (Figure 7a) generated from 4-deuterio-3-iodopyridine. The large difference between the coupling constants of the protons 2 and 4 is still surprising.

As expected, the triplet-of-triplet pattern observed with 4-pyridyl radicals (Figure 4) is quite similar to that observed with para-deuterated phenyl radicals.³ The large triplet structure with a spacing of 19 G is assigned to the protons 3 and 5 and the smaller triplet of 10 G to the protons 2 and 6. Here the almost complete absence of the coupling to the nitrogen nucleus is to be noted.

Photolysis of Pyridyl Radicals

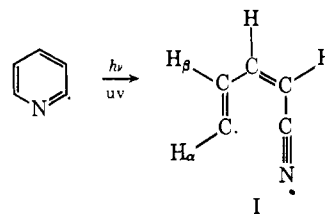
2-Pyridyl Radicals. Shown in Figure 5 is an esr spectrum obtained when an argon matrix containing 2-iodopyridine alone is irradiated with uv. Close inspection and comparison of several such spectra obtained from different matrices lead us to conclude that the spectrum is essentially a doublet of doublets complicated by the presence of varying amount of the triplet signal due to 2-pyridyl radicals as illustrated in the figure.

Irradiation with uv of an argon matrix containing 2-pyridyl radicals generated by the electron-transfer technique immediately resulted in a decrease of the signal due to 2-pyridyl radicals and an appearance of the signal with the doublet-of-doublet pattern. After 10 min of irradiation the spectrum appeared identical with that obtained by direct photolysis of the iodide.

We propose that the following photolysis reaction is responsible for the observed change. The spectrum with the doublet-of-doublet pattern is assigned to I.

(11) K. Tsuji, H. Yoshida, and K. Hayashi, *J. Chem. Phys.*, **45**, 2894 (1966).

(12) P. H. Kasai, unpublished result.



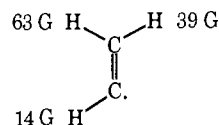
The assessed coupling constants and the g value are

$$A_{\text{iso}}(\text{H}_{\alpha}) = 18 \pm 1 \text{ G}$$

$$A_{\text{iso}}(\text{H}_{\beta}) = 56 \pm 2 \text{ G}$$

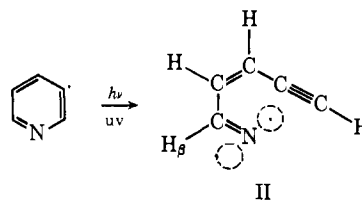
$$g = 2.001 \pm 0.001$$

The radical I may be considered as a substituted vinyl radical. The isotropic coupling constants to various protons in the vinyl radical are¹³



The proximities of the coupling constants assigned to the α and β protons in I to those of the corresponding protons in the vinyl radical are notable. The radical I was found to be stable against further irradiation with uv light.

3-Pyridyl Radicals. Shown in Figure 6 is an esr spectrum obtained when an argon matrix containing 3-iodopyridine alone is irradiated with uv for 10 min. The spectrum is concluded to be a superposition of the spectrum with a doublet-of-triplet pattern and the spectrum of 3-pyridyl radicals as illustrated in the figure. Irradiation with uv of an argon matrix containing 3-pyridyl radicals generated by the electron-transfer process resulted in a decrease of the pyridyl signal and an appearance of the signal with the doublet-of-triplet pattern. The large isotropic doublet coupling in the latter pattern suggests a presence of a proton similar to the vinyl β protons. The triplet feature is due to the ^{14}N nucleus, and the unique anisotropy ($A_{\parallel} \gg A_{\perp} \cong 0$) of this hfs indicates that the spin density is in the p_{π} orbital. The observed change, therefore, is attributed to the following photolysis.



Thus the hyperfine and the g tensors assigned to the radical II are

$$A_{\text{iso}}(\text{H}_{\beta}) = 78 \pm 2 \text{ G}$$

$$A_{\parallel}({}^{14}\text{N}) = 35 \pm 1 \text{ G}$$

$$A_{\perp}({}^{14}\text{N}) = 0 \pm 3 \text{ G}$$

$$g_{\parallel} = 2.002 \pm 0.001$$

$$\Delta g = g_{\perp} - g_{\parallel} = 0.0012 \pm 0.0002$$

(13) E. L. Cochran, F. J. Adrian, and V. A. Bowers, *J. Chem. Phys.*, **40**, 213 (1964).

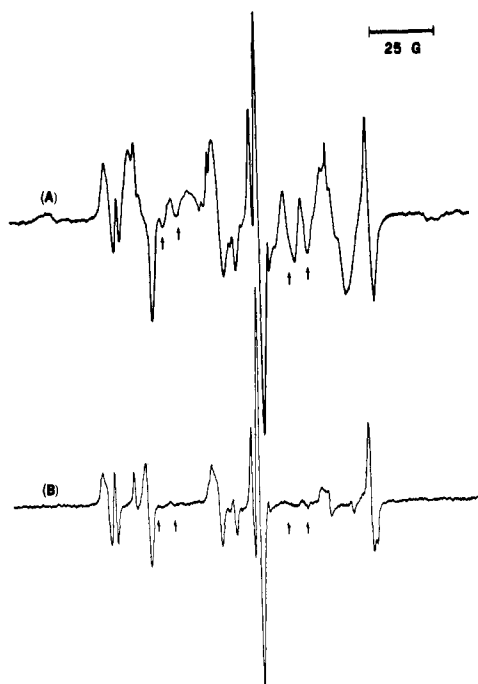


Figure 8. (A) ESR spectrum of an argon matrix containing 3-iodopyridine observed after 50 min irradiation with uv. Note the change from Figure 6A. (B) ESR spectrum of butatrienyl radical $\text{H}_2\text{C}=\text{C}=\text{C}=\dot{\text{C}}\text{H}$, generated in an argon matrix by addition of H atom to diacetylene. The arrows indicate the signals which are most likely due to $\text{HC}=\text{CHC}\equiv\text{CH}$.

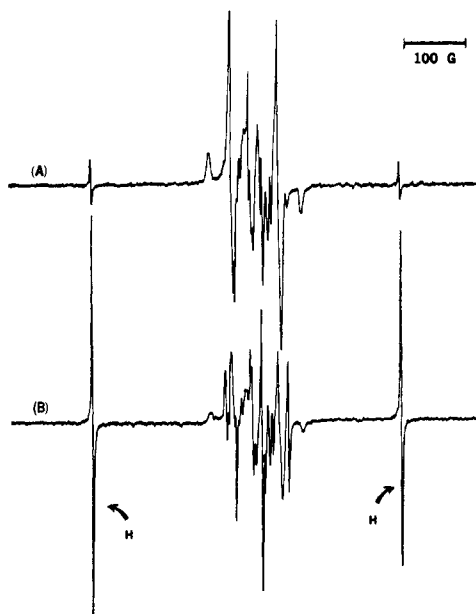


Figure 9. ESR spectrum (scanned over 600 G) of an argon matrix containing 3-iodopyridine observed after 10 min (A) and 60 min (B) of uv irradiation. Note the increase of the H-atom signals during the second irradiation.

The magnitude of Δg was assessed from the separation between the center of the "parallel" signals and that of the "perpendicular" signals (see Figure 6C). As expected, the coupling constants are very similar to those reported for the methylene imino radicals, $\text{H}_2\text{C}=\dot{\text{N}}$, for which $A_{\text{iso}}(\text{H}) = 87$ G, $A_{\parallel}({}^{14}\text{N}) = 43$ G, and $A_{\perp}({}^{14}\text{N}) \cong 0$ G.¹⁴

(14) E. L. Cochran, F. J. Adrian, and V. A. Bowers, *J. Chem. Phys.*, **36**, 1938 (1962).

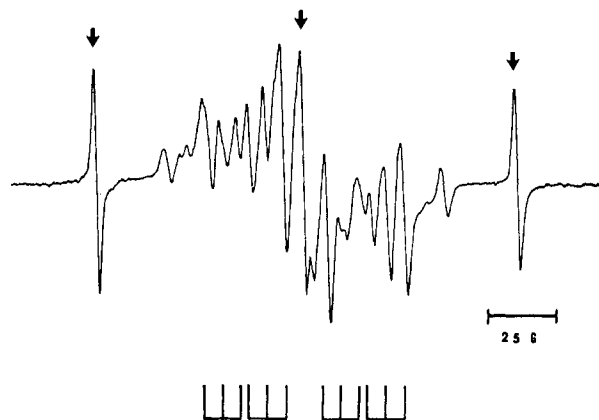
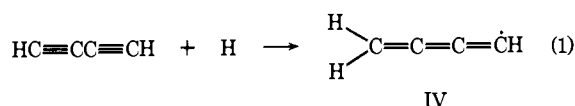
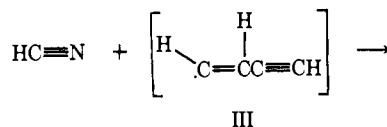
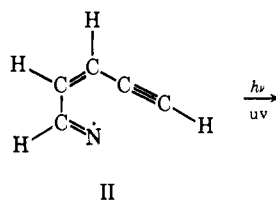


Figure 10. ESR spectrum of an argon matrix containing 4-deuterio-3-iodopyridine obtained after 60 min of uv irradiation. Note the difference from Figure 7B and the appearance of the signals due to D atoms (indicated by the arrows). Indicated below is the splitting pattern expected for $\text{HDC}=\text{C}=\text{C}=\dot{\text{C}}\text{H}$.

In order to confirm (1) the unexpected large difference between the coupling constants to the protons 2 and 4 in 3-pyridyl radicals and (2) the equally unexpected ring opening proposed above, the experiment was repeated using 4-deuterio-3-iodopyridine. According to the reaction sequence, and the assignments set forth, there should be a large effect of the deuteration upon the esr spectrum of 3-pyridyl radicals. The esr spectrum of the radical II, on the other hand, should be little affected. Such are indeed found to be the case in the spectra obtained (Figures 7A and 7B).

Most interestingly we found that the radicals II can be photolyzed further. Figure 8A shows the spectrum obtained when a matrix containing the radicals II (hence showing the spectrum in Figure 6) is further irradiated with uv for additional 60 min. It is compared with the spectrum (Figure 8B) of the butatrienyl radicals ($\text{H}_2\text{C}=\text{C}=\text{C}=\dot{\text{C}}\text{H}$) generated by the addition of hydrogen atom to diacetylene ($\text{HC}\equiv\text{CC}\equiv\text{CH}$) within an argon matrix.¹⁵ The similarity of the two spectra is conspicuous. The identity of the new radical product with the hydrogen adduct of diacetylene suggests the reaction sequence of eq 1.

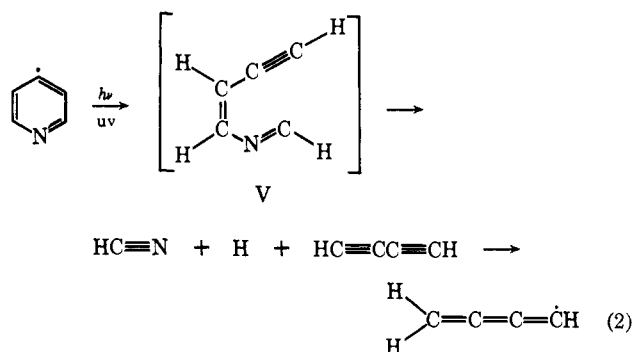


A fast, if not spontaneous, decomposition of III into a hydrogen atom and diacetylene, instead of an

(15) P. H. Kasai, L. Skattebøl, and E. B. Whipple, *J. Amer. Chem. Soc.*, **90**, 4509 (1968).

intramolecular hydrogen transfer to yield IV directly, is supported by the fact that the esr signal due to hydrogen atoms increases dramatically during the second irradiation (Figure 9). The spectrum obtained after prolonged irradiation of a matrix containing 4-deuterio-3-pyridyl radicals is shown in Figure 10. The signals due to deuterium atoms are readily recognized. The remaining part of the spectrum shows the expected large difference from the spectrum in Figure 8B. It is compared with the pattern based upon the calculated isotropic coupling constants of $\text{HDC}=\text{C}=\text{C}=\dot{\text{C}}\text{H}$. No detailed analysis of this spectrum was made.

4-Pyridyl Radicals. Figures 11A and 11B are the spectra obtained after an argon matrix containing 4-iodopyridine had been irradiated with uv for 10 and 60 min, respectively. The spectrum 11A is essentially that of 4-pyridyl radicals (see Figure 4). The spectrum 11B, however, indicates a substantial conversion of the pyridyl radicals into the butatrienyl radicals. We conclude, therefore, that 4-pyridyl radicals are much more stable than other pyridyl radicals but eventually yield to the sequence of reactions shown in eq 2. Attempts



to recognize the spectrum due to V were not successful. It must spontaneously decompose into the final products owing to the endothermicity of the step leading to its formation.

Discussion

Table I shows the g values and the coupling constants of pyridyl radicals assessed from the spectra observed in this study. The table also shows the coupling constants obtained from the results of INDO¹⁶ and EHT¹⁷ molecular orbital calculations. The structural parameters used for these calculations are $r_{\text{N-C}} = 1.34 \text{ \AA}$, $r_{\text{C-C}} = 1.39 \text{ \AA}$, and $r_{\text{C-H}} = 1.08 \text{ \AA}$. These are taken from the structure of pyridine reported by Bak, *et al.*¹⁸ The isotropic coupling constant A_{iso} to the i th atom is calculated from the spin density ρ at the valence s -atomic orbital of that atom using the relation

$$A_{\text{iso}} = Q\rho$$

where

$$Q = (8\pi/3)g_e\beta_e g_n\beta_n |\Psi(0)|^2_{\text{valence } s \text{ orbital}}$$

The values of Q used are those obtained from the atomic wave functions and are 508, 1130, and 552 G for the hydrogen $1s$, the carbon $2s$, and the nitrogen $2s$ orbitals, respectively.¹⁹ For the INDO calculation the spin

(16) J. A. Pople, D. L. Beveridge, and P. A. Dobosh, *J. Chem. Phys.*, **47**, 2026 (1967); *J. Amer. Chem. Soc.*, **90**, 4201 (1968).

(17) R. Hoffmann, *J. Chem. Phys.*, **39**, 1307 (1963).

(18) B. Bak, L. Hansen-Hygaard, and J. Rastrup-Andersen, *J. Mol. Spectrosc.*, **2**, 361 (1958).

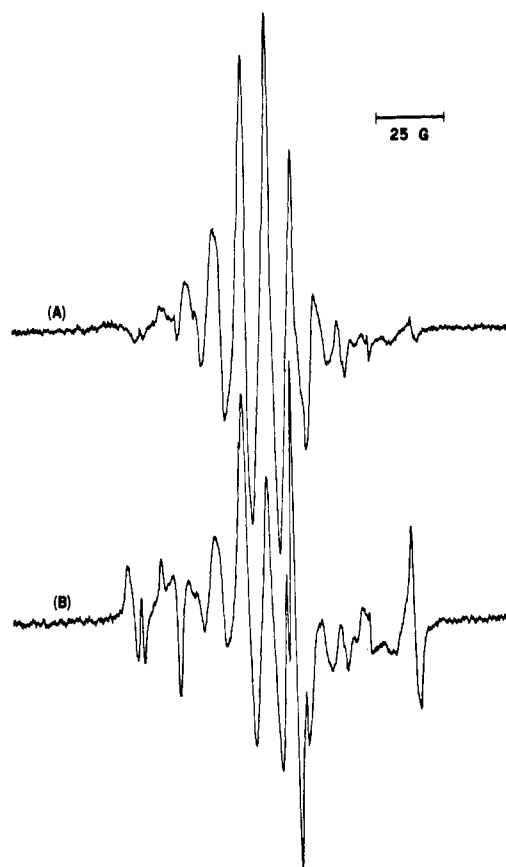


Figure 11. ESR spectrum of an argon matrix containing 4-iodopyridine observed after 10 min (A) and 60 min (B) of uv irradiation. Note the growth of the signals due to butatrienyl radicals during the second irradiation.

density ρ at an atomic orbital ϕ_i is defined as the difference in the diagonal elements of the density matrices for the α - and β -spin electrons summed over all the occupied orbitals. Thus

$$\rho_i = R_{ii}^\alpha - R_{ii}^\beta$$

where

$$R_{ii}^\alpha = \sum_j^{\text{occ MO}} (C_{ij}^\alpha)^2, \text{ etc.}$$

Here C_{ij}^α is the coefficient of the atomic orbital ϕ_i in the j th molecular orbital having α spin.

The agreement between the observed values and the result of the EHT calculations is decisively poorer. The EHT calculation employed presently, however, uses a Slater exponent of 1.0 for hydrogen. It has been shown that the EHT method would yield a much more reasonable set of hyperfine coupling constants if one uses a Slater exponent of 1.2 for hydrogen and empirically determined, much larger values for Q .²⁰ These modifications, however, would not affect the relative magnitudes of the coupling constants. Thus the discrepancies noted in the cases of 3- and 4-pyridyl radicals, between the trends of the observed coupling constants, and those predicted by the EHT method are serious. It clearly indicates a danger of utilizing the result of a

(19) See, for example, P. W. Atkins and M. C. R. Symons, "The Structure of Inorganic Radicals," Elsevier, New York, N. Y., 1967, p 21.

(20) R. E. Cramer and R. S. Drago, *J. Amer. Chem. Soc.*, **90**, 4790 (1968).

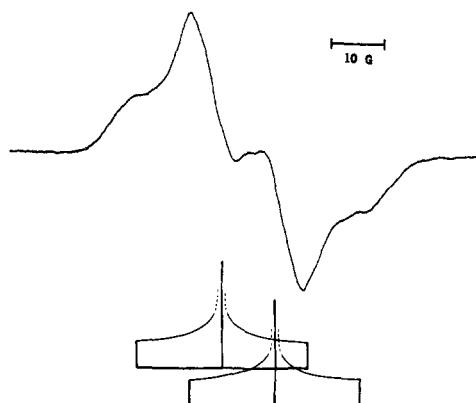
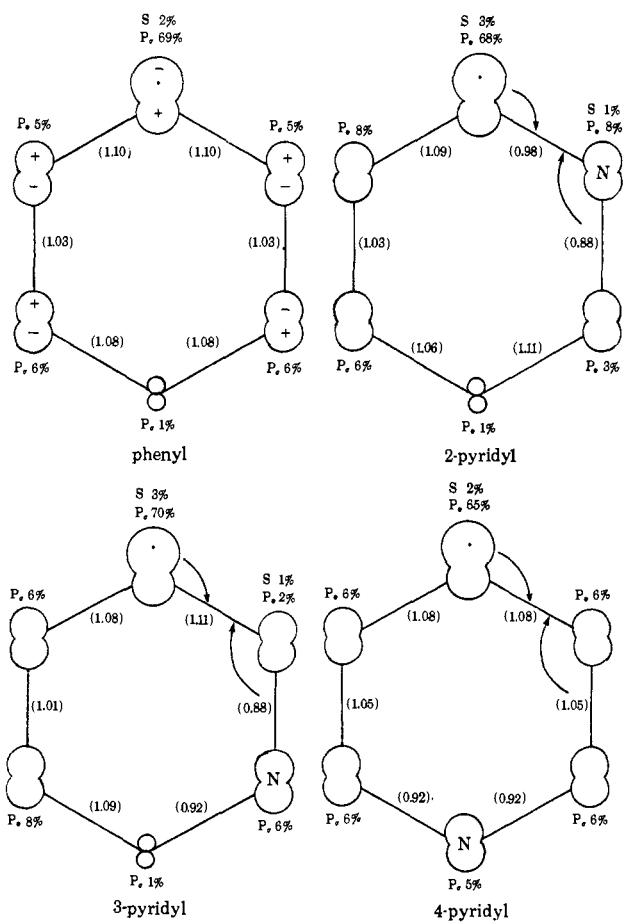


Figure 12. ESR spectrum of pyridine anion radicals generated in an argon matrix by the photoelectron transfer process. The observed signal is consistent with the anisotropic absorption pattern computed from the known isotropic coupling constants [C. L. Talcott, and R. J. Myers, *Mol. Phys.*, **12**, 549 (1967)]. The dominant feature is determined by a highly anisotropic coupling tensor to ^{14}N , and a large isotropic coupling tensor to the para proton.

one-electron orbital calculation for predicting the coupling constants of a σ radical of this type. A similar discrepancy is encountered in the case of phenyl radicals.³

The results of the INDO and the EHT calculations are in good agreement in predicting that all the pyridyl radicals are σ radicals and that the semifilled orbital in each case is mostly (60–70%) the nonbonding ρ orbital at the broken bond. The failure of EHT in predicting the correct trend of the coupling constants stems mainly from its inability to consider the spin polarization of the lower filled orbitals. Depicted below are



the LCAO descriptions of the semifilled orbitals of the phenyl, 2-, 3-, and 4-pyridyl radicals given by EHT, respectively. The numbers inside the parentheses are the total overlap populations between the neighboring first row atoms. It is immediately clear that the semifilled orbitals of pyridyl radicals are quite similar to that of the phenyl radical. The apparent large differences in the ESR spectra of these radicals are caused by the high sensitivity of the spectra to what is actually a small change in the spin density distribution. Inspection of these orbitals also reveals that the interaction between the nonbonding, broken-bond orbital and the nitrogen lone-pair orbital is rather small, though its effect is clearly manifested in the cases of 2- and 4-pyridyl radicals. The small interaction is due to a large difference between the energies of the two orbitals. The orbital energies (eV) calculated by EHT are, for example

N lone pair in pyridine	Semifilled orbitals in			
	phenyl	2-pyridyl	3-pyridyl	4-pyridyl
-12.47	-10.77	-10.62	-11.05	-10.60

The arrows in the orbital pictures depicted above indicate the rearrangement of the orbitals leading to the observed openings of the pyridyl rings under uv irradiation. Experimentally it was found that the 4-pyridyl radical is more stable against such photolysis than the 2- or 3-pyridyl radical. This is consistent with the magnitudes of the overlap populations shown above. The observed ring opening of the 2- and 3-pyridyl radicals involves a rupture of the weakest bond in the ring, while such is not the case with the 4-pyridyl radical.

What is the exact nature of the photoexcitation that leads to the opening of these radicals? Several electronic transitions are possible for these radicals in the visible and uv range. They are the $\pi \rightarrow n(c)$, $n(c) \rightarrow \pi^*$, and $n(N) \rightarrow \pi^*$ transitions, where $n(c)$ and $n(N)$ stand for the nonbonding orbitals of the broken bond and the nitrogen lone pair, respectively. The first two transitions, $\pi \rightarrow n(c)$ and $n(c) \rightarrow \pi^*$, are expected to be close to the corresponding transitions of phenyl radicals. Porter and Ward identified the $\pi \rightarrow n(c)$ transition of phenyl radicals at $\sim 5000 \text{ \AA}$ and saw no other transition in the range covered (2900–7000 \AA).¹ Thus it is unlikely that the $n(c) \rightarrow \pi^*$ transition of phenyl or pyridyl radicals falls within the range of uv (2500–4000 \AA) used in our experiment. Irradiation of matrices containing pyridyl radicals with light above 4000 \AA did not produce any ring opening. The $n(N) \rightarrow \pi^*$ transition of pyridine, on the other hand, occurs at 2500–3000 \AA .²¹ We propose, therefore, that the $n(N) \rightarrow \pi^*$ excitation is the initial step leading toward the ring opening of pyridyl radicals. We do not believe, however, that a mere promotion of an electron into the π^* level is sufficient to cause the opening. The pyridine anion radicals generated in an argon matrix by the photoelectron transfer process are found to be quite stable under uv irradiation (Figure 12). We must conclude that the existence of a semifilled, nonbonding orbital which would permit the formation of a triple bond in the final product is also required.

Irradiation of an argon matrix containing phenyl

(21) G. Herzberg, "Electronic Spectra of Polyatomic Molecules," Van Nostrand, Princeton, N. J., 1967, p 554.

radicals with shorter uv (1500–2000 Å) obtained from a xenon microwave discharge unit did not alter its esr spectrum.

Acknowledgment. The authors wish to thank Drs. E. Hedaya and L. Skattebøl for their stimulating discussions and kind supply of 2- and 4-iodopyridines.

Crystal and Molecular Structure of Bis(dimethylglyoximato)diimidazoleiron(II)–Dimethanol

K. Bowman, A. P. Gaughan, and Z. Dori*¹

Contribution from the Department of Chemistry, Temple University of the Commonwealth System of Higher Education, Philadelphia, Pennsylvania 19122. Received May 8, 1971

Abstract: The crystal and molecular structure of bis(dimethylglyoximato)diimidazoleiron(II)–dimethanol ($\text{Im}_2\text{Fe}(\text{DMG})_2 \cdot 2\text{CH}_3\text{OH}$) has been determined from the intensities of 1061 unique observed reflections collected by counter techniques. The complex crystallizes in the monoclinic space group $P2_1/c$ with unit cell dimensions $a = 8.217$ (3), $b = 10.534$ (3), $c = 13.260$ (5) Å, and $\beta = 94.85$ (3)°; $d_{\text{measd}} = 1.42$ (3) g/cm³, $d_{\text{calcd}} = 1.41$ g/cm³ for $Z = 2$. The structure was solved by the heavy atom method and refined by full-matrix least-squares methods to a conventional $R = 0.052$ and weighted $R = 0.058$. The complex is centrosymmetric and the iron atom is bound to six nitrogen atoms in a tetragonally distorted octahedral configuration. The O···O contact between the two dimethylglyoxime ligands is 2.588 (8) Å. There is a hydrogen bond between each pair of oxygen atoms and the two O–H distances are 1.0 (1) and 1.5 (1) Å. The O–H···O angle is 159 (4)°. The two N–O distances are significantly different (1.408 (7) and 1.365 (7) Å) resulting from the asymmetry of the hydrogen bond with the longer N–O distance being associated with the shorter O–H bond length. The equatorial Fe–N distances are 1.893 (6) and 1.918 (6) Å and the axial Fe–N bond length is 1.985 (5) Å. In the absence of steric interference between the imidazole hydrogens and the DMG ligands, the axial Fe–N bond distance can be taken as the one to be expected for Fe(II) bound to an axial imidazole.

One of the most interesting and yet unsolved problems of biochemistry is the question of the reversible uptake of molecular oxygen and the cooperative effect observed for this process in hemoglobin. There is little known about the special structural factors in oxygen-carrying complexes since investigations are hampered by the high molecular weight protein portion. There is therefore great interest in low molecular weight metal complexes whose structures resemble those of iron porphyrins. Such model compounds are required to possess unsaturated equatorial ligands containing nitrogen donor atoms and biologically important axial ligands. One such complex is bis(dimethylglyoximato)diimidazoleiron(II) ($\text{Im}_2\text{Fe}(\text{DMG})_2$).

Although we fully realize that dimethylglyoxime is not a porphyrin ring,^{2a} we feel that important structural information can be obtained from such a complex, particularly with regard to the iron–imidazole configuration. In this paper we report the results of the structural determination of the title compound.^{2b}

Experimental Section

The crystals were prepared in a special vessel constructed from two 500-ml erlenmeyer flasks connected by a sintered glass frit of

medium porosity. During the entire experiment both of the compartments were kept under purified nitrogen. In the first compartment 0.50 g (0.0014 mol) of ferrous perchlorate hexahydrate, 0.33 g (0.0028 mol) of dimethylglyoxime, and 0.19 g (0.0028 mol) of imidazole were placed in 150 ml of dimethylformamide. The second compartment contained 10.9 g (0.0042 mol of tetrabutylammonium hydroxide) of a 10% by weight solution of tetrabutylammonium hydroxide in methanol in 450 ml of methanol. The two compartments were closed under nitrogen and the pressure was adjusted to allow a slow diffusion from the second compartment into the first compartment. After 1 week analytically pure deep red crystals suitable for X-ray diffraction studies were obtained from the first compartment. *Anal.* Calcd for $\text{Im}_2\text{Fe}(\text{DMG})_2 \cdot 2\text{CH}_3\text{OH}$: C, 39.52; H, 6.21; N, 23.03. Found:³ C, 40.37; H, 6.26; N, 23.10.

The space group and approximate unit cell dimensions were determined from preliminary precession and Weissenberg photographs using Ni-filtered Cu K α radiation. The observed extinctions, $h0l, l \neq 2n$, and $0k0, k \neq 2n$, suggested the centrosymmetric space group $P2_1/c$ (C_{2h}^2 , no. 14).

A small crystal (0.22 × 0.25 × 0.18 mm) in the form of a parallelepiped was chosen and mounted with its a^* axis coincident with the ϕ axis of a G.E. Quarter Circle Orienter incorporated into a G.E. XRD-6 diffractometer system. The air-sensitive crystal was coated with spray varnish to prevent decomposition. All measurements were made at 25° at a take-off angle of 3° with Zr-filtered Mo K α radiation ($\lambda = 0.7107$ Å). A least-squares refinement⁴ of accurately measured angular settings for 23 reflections gave the following unit cell parameters: $a = 8.217$ (7), $b = 10.534$ (3), $c = 13.260$

(1) Direct correspondence to Zvi Dori, Department of Chemistry, Technion-Israel Institute of Technology, Haifa, Israel.

(2) (a) Cobaloxime, for example, successfully mimics the chemistry of vitamin B₁₂: G. N. Schrauzer, *Accounts Chem. Res.*, **1**, 97 (1968). (b) The structure of bis(cyclohexane-1,2-dioximato)diimidazoleiron(II) dihydrate was reported by Prout [C. K. Prout and T. J. Wiseman, *J. Chem. Soc. A*, 497 (1964)], but because of disorder in the cyclohexyl rings the important structural parameters are not accurately known.

(3) Microanalyses were performed by the Schwarzkopf Microanalytical Laboratory, Woodside, N. Y. 11377.

(4) In addition to the PICKLIST setting program, the main programs used in this work were local modifications of the Busing–Levy ORFLS least-squares program, the Zalkin FORDAF Fourier program, the Busing–Martin–Levy ORFFE function and error program, and the Johnson ORTEP plotting program. Various other local programs were also used. All computing was performed on the Temple University CDC 6400 computer.